

Higgs boson footprints of hefty ALPs

Anisha,^{1,*} Supratim Das Bakshi,^{2,†} Christoph Englert,^{1,‡} and Panagiotis Stylianou^{3,§}
¹*School of Physics and Astronomy, University of Glasgow, Glasgow G12 8QQ, United Kingdom*
²*CAFPE and Departamento de Física Teórica y del Cosmos, Universidad de Granada, Campus de Fuentenueva, E-18071 Granada, Spain*
³*Deutsches Elektronen-Synchrotron DESY, Notkestr. 85, 22607 Hamburg, Germany*



(Received 12 July 2023; accepted 19 October 2023; published 20 November 2023)

We discuss axionlike particles (ALPs) within the framework of Higgs effective field theory, targeting instances of close alignment of ALP physics with a custodial singlet character of the Higgs boson. We tension constraints arising from new contributions to Higgs boson decays against limits from high-momentum transfer processes that become under increasing control at the LHC. Going beyond leading-order approximations, we highlight the importance of multitop and multi-Higgs production for the pursuit of searches for physics beyond the Standard Model extensions.

DOI: [10.1103/PhysRevD.108.095032](https://doi.org/10.1103/PhysRevD.108.095032)

I. INTRODUCTION

Searches for new interactions beyond the Standard Model of particle physics have, so far, been unsuccessful. This is puzzling as the Standard Model contains a plethora of flaws that are expected to be addressed by a more comprehensive theory of microscopic interactions. A reconciliation of these flaws can have direct phenomenological consequences for physics at or below the weak scale $v \simeq 246$ GeV. This is particularly highlighted by fine-tuning problems related to the Higgs mass or the neutron electric dipole moment, both of which take small values due to cancellations which are not protected by symmetries in the Standard Model (SM). Dynamical solutions to these issues have a long history, leading to new interactions and states around the TeV scale to address Higgs naturalness, or relaxing into and CP -conserving QCD vacuum via a Peccei-Quinn-like mechanism [1]. Often such approaches yield an additional light pseudo-Nambu Goldstone field, in the guise of a composite Higgs boson or the axion [2].

The search for a wider class of the latter states referred to as axionlike particles (ALPs) bridges different areas of high energy physics. Efforts to detect ALPs across different mass and coupling regimes have shaped the current

BSM programme in many experimental realms (see, e.g., [3,4] for recent reviews). In particular, at the Large Hadron Collider (LHC), ALP interactions have been discussed in relation to their telltale signatures arising from $\sim F\tilde{F}$ coupling structures [5], top quarks [6], emerging signatures [7], flavor physics [8,9], electroweak precision constraints [10], Higgs decays [10,11], and mixing [12]. The methods of effective field theory [13] naturally embed ALP-related field theories into a broader framework of a more modern perspective on renormalizability [14–16].

Experimental searches for these states have been carried out using a variety of techniques, including collider searches, precision measurements of atomic and nuclear transitions (e.g., ACME [17] and nEDM [18]), and searches from astrophysical events [19,20], over a wide range of ALP mass [21]. In particular for the ALP mass range $M_A \in \text{GeV}$, the most stringent exclusion limits for ALPs are derived from ultraperipheral lead nuclei collision data [22,23]. These limits are from exclusive diphoton searches, and define SM–ALPs interactions via electromagnetic interactions ($\sim F\tilde{F}$).¹ The ATLAS limits [22] on the ALP–photon cross sections when put in terms of ALP–photon couplings is found in the range $g_{A\gamma} \in [0.05, 1] \text{ TeV}^{-1}$ [24]. However, in general, the ALP–SM interactions can be defined via gauge bosons, fermions, and scalars; although, its decays will depend on its mass. The limits on ALP couplings to the SM fields (except photons) are less stringent (e.g. see Ref. [25]). The exotic decays of

*anisha@glasgow.ac.uk

†sdb@ugr.es

‡christoph.englert@glasgow.ac.uk

§panagiotis.stylianou@desy.de

Published by the American Physical Society under the terms of the [Creative Commons Attribution 4.0 International license](https://creativecommons.org/licenses/by/4.0/). Further distribution of this work must maintain attribution to the author(s) and the published article's title, journal citation, and DOI. Funded by SCOAP³.

¹When the ALP mass $M_A < 2m_e$, only the di-photon channel is the allowed decay process via SM particles. In same manner, with greater ALP mass, the decay modes to other leptons, quarks (jets), gauge bosons open up as well.

the SM Higgs and Z-bosons are promising channels for ALP searches (particularly benefiting from the high-luminosity run of the LHC), e.g., with the decay modes $h \rightarrow ZA$ [26].

It is the latter perspective that we adopt in this note to focus on ALP interactions with the Higgs boson, also beyond leading order. Adopting the methodology of Higgs effective theory (HEFT), we can isolate particular interactions of the ALP state and trace their importance (and thus the potential for constraints) to representative collider processes that navigate between the low energy precision and the large momentum transfer regions accessible at the LHC. If the interactions of ALPs and Higgs particles is predominantly related to a custodial singlet realization of the Higgs boson, these areas might well be the first phenomenological environments where BSM could be unveiled as pointed out in, e.g., Ref. [27]. In parallel, our results demonstrate the further importance of multitop and multi-Higgs final states as promising candidates for the discovery of new physics. With the LHC experiments closing in on both Higgs pair [28,29] and four-top production in the SM [30,31], such searches becoming increasingly interesting for our better understanding of the BSM landscape.

This work is organized as follows: In Sec. II, we review the ALP-HEFT framework that we use in this study to make this work self-contained (a comprehensive discussion is presented in [27]). In Sec. III, we focus on the decay phenomenology of the Higgs boson in the presence of ALP interactions before we turn to discuss *a priori* sensitive processes that can provide additional constraints due to their multiscale nature and kinematic coverage. Specifically, in Sec. IV we analyze ALP corrections to Higgs propagation as accessible in four-top final states [31–33], which informs corrections to multi-Higgs production. We conclude in Sec. V.

II. ALP CHIRAL HEFT LAGRANGIAN

The leading order ALP interactions with SM fields in the framework of chiral (nonlinear) electroweak theory are written as

$$\mathcal{L}_{\text{LO}} = \mathcal{L}_{\text{LO}}^{\text{HEFT}} + \mathcal{L}_{\text{LO}}^{\text{ALP}}. \quad (1)$$

$\mathcal{L}_{\text{LO}}^{\text{HEFT}}$ is the chiral dimension-2 HEFT Lagrangian [34–38]. In this framework, the SM Higgs (H) is a singlet field and the Goldstone bosons π^a are parametrized nonlinearly using the matrix U

$$U(\pi^a) = \exp(i\pi^a \tau^a / v), \quad (2)$$

with τ^a as the Pauli matrices with $a = 1, 2, 3$ and $v \simeq 246$ GeV. The U matrix transforms under $L \in SU(2)_L$, $U(1)_Y \subset SU(2)_R \ni R$ as $U \rightarrow LUR^\dagger$ and is expanded as

$$U(\pi^a) = \mathbb{1}_2 + i\frac{\pi^a}{v}\tau^a - \frac{2G^+G^- + G^0G^0}{2v^2}\mathbb{1}_2 + \dots, \quad (3)$$

where $G^\pm = (\pi^2 \pm i\pi^1)/\sqrt{2}$ and $G^0 = -\pi^3$. The dynamics of the gauge bosons W_μ^a and B_μ are determined by the usual $SU(2)_L \times U(1)_Y$ gauge symmetry. Weak gauging of $SU(2)_L \times U(1)_Y$ is achieved through the standard covariant derivative

$$D_\mu U = \partial_\mu U + ig_W(W_\mu^a \tau^a / 2)U - ig'UB_\mu \tau^3 / 2. \quad (4)$$

The gauge fields in the physical (mass and electromagnetic $U(1)_{\text{em}}$) basis are related to the gauge basis via the Weinberg angle $s_W = \sin \theta_W$, $c_W = \cos \theta_W$

$$W_\mu^\pm = \frac{1}{\sqrt{2}}(W_\mu^1 \mp W_\mu^2),$$

$$\begin{pmatrix} Z_\mu \\ A_\mu \end{pmatrix} = \begin{pmatrix} c_W & s_W \\ -s_W & c_W \end{pmatrix} \begin{pmatrix} W_\mu^3 \\ B_\mu \end{pmatrix}. \quad (5)$$

The leading order HEFT Lagrangian relevant for our discussion is then given by

$$\mathcal{L}_{\text{LO}}^{\text{HEFT}} = -\frac{1}{4}W_{\mu\nu}^a W^{a\mu\nu} - \frac{1}{4}B_{\mu\nu}B^{\mu\nu} + \mathcal{L}_{\text{ferm}} + \mathcal{L}_{\text{Yuk}}$$

$$+ \frac{v^2}{4}\mathcal{F}_H \text{Tr}[D_\mu U^\dagger D^\mu U] \quad (6a)$$

$$+ \frac{1}{2}\partial_\mu H \partial^\mu H - V(H). \quad (6b)$$

The interactions of the singlet Higgs field with gauge and Goldstone bosons are parametrized by the flare function \mathcal{F}_H given as

$$\mathcal{F}_H = \left(1 + 2(1 + \zeta_1)\frac{H}{v} + (1 + \zeta_2)\left(\frac{H}{v}\right)^2 + \dots\right). \quad (6c)$$

The couplings ζ_i denote the independent parameters that determine the leading-order interactions of the Higgs boson with the gauge fields. $\mathcal{L}_{\text{ferm}}$ parametrizes the fermion-gauge boson interactions, which we take SM-like in the following. $V(H)$ is the Higgs potential, which we relate to the SM expectation

$$V(H) = \frac{1}{2}M_H^2 H^2 + \kappa_3 H^3 + \kappa_4 H^4. \quad (7)$$

with $\kappa_3 \simeq 32$ GeV, $\kappa_4 \simeq 0.03$ in the SM.

In this work, we consider ALP interactions that particularly probe the singlet character of the Higgs boson as a parametrized by the HEFT Lagrangian. The interactions are given by

$$\mathcal{L}_{\text{LO}}^{\text{ALP}} = \frac{1}{2}\partial_\mu \mathcal{A} \partial^\mu \mathcal{A} - \frac{1}{2}M_A^2 \mathcal{A}^2$$

$$+ a_{2D} \left(i v^2 \text{Tr}[U \tau^3 U^\dagger \mathbf{V}_\mu] \frac{\partial_\mu \mathcal{A}}{f_A} \mathcal{F}_{2D} \right) \quad (8a)$$

with

$$\mathcal{F}_{2D} = \left(1 + 2\zeta_{12D} \frac{H}{v} + \zeta_{22D} \left(\frac{H}{v} \right)^2 + \dots \right), \quad (8b)$$

and

$$\mathcal{V}_\mu = (D_\mu U) U^\dagger. \quad (8c)$$

In Eq. (8), f_A denotes the scale linked with the ALP interactions. The interactions specified by Eq. (8) are the leading order chiral interactions of the ALP field with SM states. These couplings specifically probe the custodial singlet nature of the Higgs boson [27]. Therefore, the phenomenology of these interactions provides relevant insights into the mechanism of electroweak symmetry breaking (EWSB) and its relation to axionlike states. The radiative imprints of these interactions on SM correlations are then captured by the chiral dimension-4 interactions contributing to $\mathcal{L}_{LO}^{\text{HEFT}}$ when HEFT parameters coincide with the SM expectation.²

In comparison with a linear ALP prescription, the chiral Lagrangian exhibits unique ALP-Higgs-gauge boson interactions induced from a_{2D} and additional ALP-gauge boson couplings and structures (for a detailed discussion see Ref. [27]). The fact that a_{2D} arises at leading order in the chiral prescription of EWSB compared to the linear case indicates its importance; on the one hand the phenomenology of a_{2D} is crucial for distinguishing the two approaches. On the other hand the induced interactions can be prevalent compared to effects from higher order operators in the chiral expansion. This stems from the generality of $\mathcal{F}_H \neq \mathcal{F}_{2D}$ which is not present in the linear case.

The aim of our analysis is to clarify the phenomenological reach to the couplings involved in Eq. (8) from two different angles. First, these interactions are clear indicators of a singlet character of the Higgs boson in HEFT. Second, the interactions $\sim \zeta_{12D}$ will introduce modifications to the Higgs boson propagation and Higgs decay in HEFT, ζ_{22D} will imply modifications to the Higgs pair production rate. Although the ALP might be too light to be directly accessible at collider experiments such as the LHC, its virtual imprint through specific predictions between the correlations of four-top and Higgs pair production could reveal its presence. We will turn to the expected constraints in the next section. Throughout, we will identify the HEFT parameters with their corresponding tree-level SM limit except for the deviations introduced by the ALP, which we also detail below. We will focus on the interactions that are generated at order $a_{2D}\zeta_{12D}$, etc.; fits against the ALP-less HEFT (or the SM as a particular HEFT parameter choice) should be sensitive to these contributions when data is

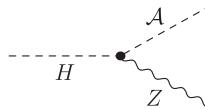
²All interactions detailed above are implemented using the FeynRules package [39,40].

consistent with the latter expectation. To reflect this we will therefore also assume that HEFT operators coincide with their SM expectation. Specifically this means that we will choose vanishing HEFT parameters arising at chiral dimension-4. Departures from the SM correlations are then directly related to (radiative) presence of the ALP.

Couplings of ALPs with other SM fields can in principle be present and sizeable (potentially with equivalent insertions in the linear EWSB) leading to signs of new physics in processes beyond the ALP-Higgs interactions we consider.³ Such other processes however will not have the discriminative power to pinpoint to the nature of EWSB. Thus, the assumption of including only the leading order a_{2D} interaction allows us center our attention to identifying the most prominent processes for our aim.

III. DIRECT CONSTRAINTS FROM HIGGS DECAYS

The interactions of an ALP with a Higgs boson via the $a_{2D}\zeta_{12D}$ coupling of Eq. (8) is tree-level mediated. The exotic decay of the Higgs boson via $H \rightarrow AZ$ at leading order is given by



$$= -2i \frac{e}{c_W s_W} \frac{v}{f_A} a_{2D} \zeta_{12D} q^\mu(H), \quad (9)$$

with $q^\mu(H)$ denoting the four-momentum carried by the Higgs leg. When kinematically accessible, the decay width of the Higgs boson receives a non-SM contribution

$$\begin{aligned} \Gamma(H \rightarrow AZ) &= \frac{v^2 a_{2D}^2 \zeta_{12D}^2}{274 s_W^2 c_W^2 f_A^2 M_H^3 M_Z^2} \\ &\times (M_A^4 - 2M_A^2(M_H^2 + M_Z^2) \\ &+ (M_H^2 - M_Z^2)^2)^{3/2}. \end{aligned} \quad (10)$$

Assuming this two-body process as the most dominating BSM decay involving the ALP, the SM Higgs boson signal strengths get uniformly modified

$$\mu_{\text{SM},A} = \frac{\Gamma(H)_{\text{SM}}}{\Gamma(H \rightarrow AZ) + \Gamma(H)_{\text{SM}}}, \quad (11)$$

with $\Gamma(H)_{\text{SM}} \simeq 4$ MeV as the total Higgs boson decay width in the SM [41]. To constrain this BSM decay, we use the well constrained and hence representative signal strength for $H \rightarrow \gamma\gamma$. This has been measured [42]

³A potential UV completion would be the dominant coupling of the ALP to a singlet extension of the SM Higgs sector. The couplings $\sim a_{2D}$ would then be induced to the visible Higgs boson's interactions and mixing angle suppression could be (partially) compensated by a scale hierarchy $f_a < v$.

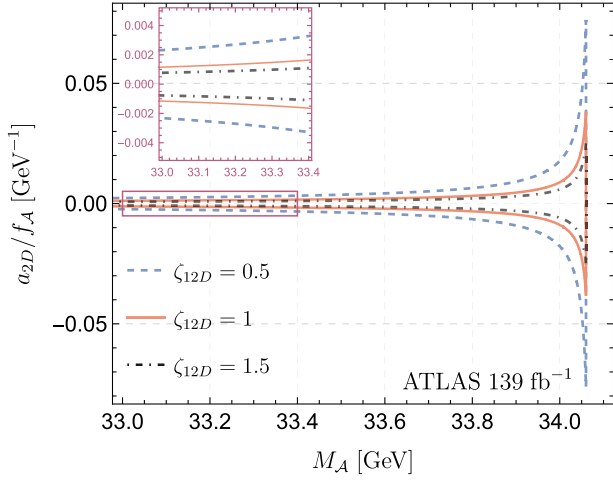


FIG. 1. The allowed parameter region obtained from the diphoton signal strength reported by ATLAS for their 139 fb⁻¹ dataset for different values of ζ_{12D} .

$$\mu_{\gamma\gamma} = 1.04_{-0.09}^{+0.1} \quad (12)$$

for the representative ATLAS Run 2 dataset of 139 fb⁻¹. For the on-shell decay of $H \rightarrow AZ$, the maximum value of ALP mass allowed kinematically is $\simeq 34$ GeV with $M_H = 125$ GeV and $M_Z = 91.18$ GeV. For heavier ALP masses, the branching ratio quickly dies off due to the offshellness of the involved Z boson.

The allowed parameter space in a_{2D}/f_A vs M_A plane is shown in Fig. 1 for three different values of ζ_{12D} . The above 95% limit translates into the lower bound on $\Gamma(H \rightarrow AZ) < 0.65$ MeV using Eq. (11) for $\zeta_{12D} = 1$. The above bound on $\Gamma(H \rightarrow AZ)$ is reduced by half with the HL-LHC projections for $H \rightarrow \gamma\gamma$ at 3 ab⁻¹ [43], i.e., we obtain $\Gamma(H \rightarrow AZ) < 0.32$ MeV for $\zeta_{12D} = 1$.

IV. HIGGS SIGNALS OF VIRTUAL ALPS

A. Propagation vs. on-shell properties: Four-top production

BSM corrections to the Higgs self-energy Σ_H can give rise to an oblique correction

$$\hat{H} = -\frac{M_H^2}{2} \Sigma_H''(M_H^2), \quad (13)$$

analogously to the \hat{W} , \hat{Y} parameters in the gauge sector, e.g., [44]. Such a correction leads to a Higgs propagator modification [32]

$$-i\Delta_H(q^2) = \frac{1}{q^2 - M_H^2} \left(1 + \hat{H} \left(1 - \frac{q^2}{M_H^2} \right) \right), \quad (14)$$

indicating a departure for large momentum transfers at unit pole residue. Measurements of this parameter have by now

been established by ATLAS and CMS in Refs. [31,33]. The expected upper limit is

$$\hat{H} \leq 0.12, \quad (15)$$

at 95% Confidence Limit (C.L.) from the recent four-top production results of Ref. [31]. We can reinterpret this in the framework that we consider. In parallel, we can employ an extrapolation of four-top final states to estimate sensitivity improvements that should become available in \hat{H} -specific analyses at the high-luminosity LHC (ATLAS currently observe a small tension in their \hat{H} fit).

Explicit calculation in general R_ξ gauge of the ALP insertion of Eq. (9) into the Higgs two-point function yields the ξ -independent result (see also remarks in [36–38])

$$\Gamma(H(q)H(q)) = \frac{a_{2D}^2 \zeta_{12D}^2}{4\pi^2 f_A^2} (4M_A^4 - 3M_A^2 q^2 + (q^2 - 3M_Z^2)q^2) \Delta_{UV} + \dots, \quad (16)$$

with $\overline{\text{MS}}$ factor

$$\Delta_{UV} = \frac{\Gamma(1 + \epsilon)}{\epsilon} \left(\frac{4\pi\mu^2}{M_H^2} \right)^\epsilon \quad (17)$$

in dimensional regularization $D = 4 - 2\epsilon$ with 't Hooft mass μ . The ellipses in Eq. (16) denote finite terms for $\epsilon \rightarrow 0$ (see below).

In the following we will adopt the on-shell scheme for field and mass renormalization [cf. Eq. (14)], and the $\overline{\text{MS}}$ scheme for HEFT parameters (see also [36–38,45–47]). On the one hand, part of the divergence of Eq. (16) are then canceled by the (divergent, div.) counterterms related to the Higgs wave function and mass renormalization

$$\begin{aligned} \delta Z_H|_{\text{div}} &= \frac{3a_{2D}^2 \zeta_{12D}^2 (M_A^2 + M_Z^2)}{4\pi^2 f_A^2}, \\ \delta M_H^2|_{\text{div}} &= \frac{a_{2D}^2 \zeta_{12D}^2 (4M_A^4 - 3M_A^2 M_H^2 - 3M_H^2 M_Z^2)}{4\pi^2 f_A^2}. \end{aligned} \quad (18)$$

On the other hand, the appearance of a q^4 contribution signifies the sourcing of the chiral dimension-4 operator $\mathcal{O}_{\square\square}$ of the HEFT Lagrangian

$$\mathcal{O}_{\square\square} = a_{\square\square} \frac{\square H \square H}{v^2}. \quad (19)$$

This operator is renormalized by the ALP interactions via

$$\delta a_{\square\square} = -\frac{a_{2D}^2 \zeta_{12D}^2 v^2}{8\pi^2 f_A^2} \Delta_{UV}. \quad (20)$$

Together, the renormalized Higgs two-point function then links to the \hat{H} parameter as

$$\begin{aligned} \hat{H} = & -\frac{a_{2D}^2 M_H^2 \zeta_{12D}^2}{8\pi^2 f_A^2} (2B_0(M_H^2, M_A^2, M_Z^2)|_{\text{fin}} \\ & - 4(M_A^2 - M_H^2 + M_Z^2)B'_0(M_H^2, M_A^2, M_Z^2) \\ & + [M_A^4 - 2M_A^2(M_H^2 + M_Z^2) \\ & + (M_H^2 - M_Z^2)^2]B''_0(M_H^2, M_A^2, M_Z^2)), \end{aligned} \quad (21)$$

where “fin.” denotes the UV finite part of the Passarino-Veltman B_0 function after subtracting Eq. (17) and derivatives are taken with respect to the first argument of the B_0 function (an explicit representation can be found in Ref. [48]). \hat{H} vanishes in the decoupling limit $f_A > M_A \gg M_H$.

Equation (21) shows that propagator corrections that can be attributed to \hat{H} probe similar couplings as the Higgs decay of Eq. (10), however, in a momentum transfer-enhanced way, at the price of a loop suppression. This way the energy coverage of the LHC that becomes under increasing statistical control provides additional sensitivity beyond the fixed scale Higgs decay. Any enhanced sensitivity to the on vs. off-shell phenomenology that can be gained from the combination of the processes discussed so far, can then break the degeneracies between the different HEFT coefficients in Eq. (8b).

To obtain an extrapolation estimate from the current constraints on \hat{H} , we implement the modifications from \hat{H} in `Madgraph5_aMC@NLO` [49] in order to estimate the changes caused in the four-top cross section from different contributions to the Higgs self-energy, and extrapolate the result of Eq. (15). Assuming a significance $S(\hat{H} = 0.12)/\sqrt{B} = 2$ from the constraint of Ref. [31] at 140/fb, and then subsequently rescaling the results to 3/ab, we obtain the approximate significance at HL-LHC. While using the more recent results yields improved bounds compared to earlier projections of Ref. [50] that include systematics (due to improvements in the analysis procedure utilizing ML techniques), our projections remain conservative compared to the previously estimated significance with only statistical uncertainties, see Fig. 2.

In Fig. 3, we also see that if M_A is light, it will freely propagate in the 2 point function thus imparting the characteristic q^4 dependence probed by \hat{H} . This also means that this behavior is essentially independent of the light ALP mass scale. Turning to heavier states, this kinematic dependence is not sourced as efficiently anymore, leading to a quick decoupling from the two-point Higgs function and reduced sensitivity and larger theoretical uncertainty. We will return to the relevance of \hat{H} for the discussed scenario after discussing the modifications to Higgs pair production in the next section.

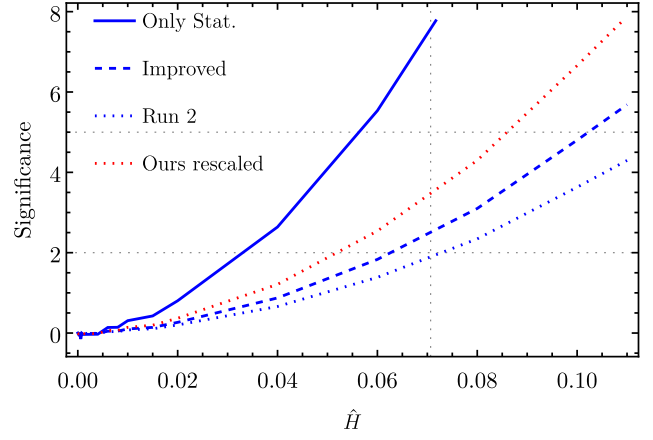


FIG. 2. Expected significance for different values of \hat{H} at HL-LHC using the projections of Ref. [50] (blue) and our estimates from projections using Eq. (15) (red).

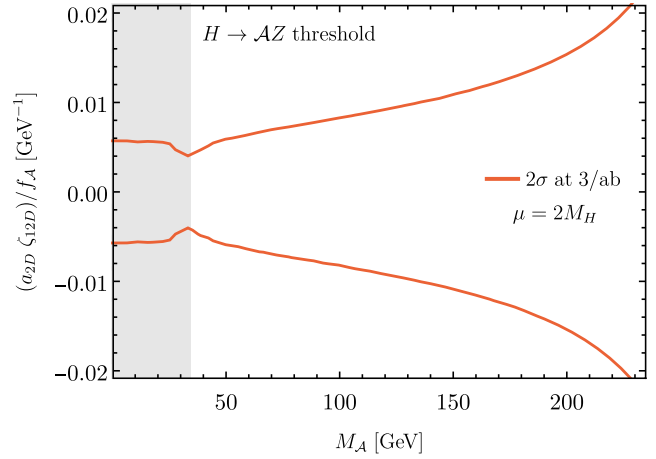


FIG. 3. The solid line indicates the 2σ contour on the $a_{2D}/f_A - M_A$ plane from the \hat{H} analysis for a scale $\mu = 2M_H$. The shaded region indicates the open $H \rightarrow AZ$ decay channel.

B. Higher terms of the ALP flare function: Higgs pair production

Corrections to Higgs pair production under the same assumptions as in the previous section are contained in propagator corrections and corrections to trilinear Higgs coupling. As with the chiral dimension-4 operator that leads to new contributions to the Higgs-two point function, there are additional operators that modify the Higgs trilinear interactions. The amputated off-shell three-point function receives contributions (see also [47])

$$\begin{aligned} v^3 \Gamma_1(H(q)H(k_1)H(k_2)) = & a_{\chi 1}(q^4 + k_1^4 + k_2^4) \\ & + 2a_{\chi 2}(q^2 k_1^2 + k_1^2 k_2^2 + q^2 k_2^2) \\ & + a_{\chi 3}v^2(q^2 + k_1^2 + k_2^2), \end{aligned} \quad (22)$$

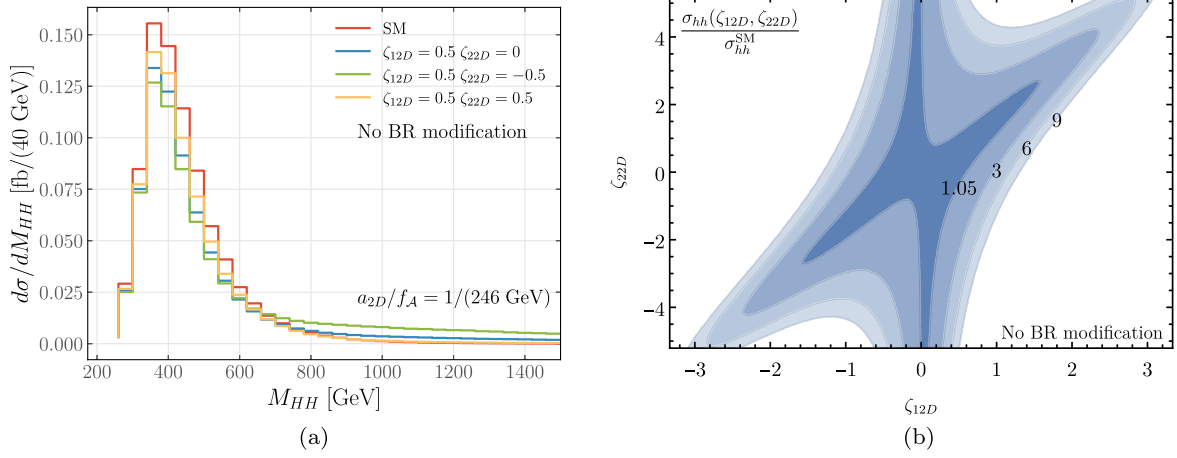


FIG. 4. Invariant mass of the Higgs pair $M_{HH}^2 = (p_{H,1} + p_{H,2})^2$ for different values of $\zeta_{12D,22D}$ and the SM in $gg \rightarrow HH$, and $M_A = 1$ GeV is shown on the left. Considering the final state Higgs boson on-shell, the corrections to their decays according to Eq. (10) are not included. The normalization is chose to $\sigma(HH)^{\text{SM}} \simeq 32$ fb [67] and we use SM K factors to qualitatively include higher order QCD corrections. Squared contributions from the renormalized $gg \rightarrow hh$ amplitude are included. On the right the ratio of the new-physics cross section with respect to the SM is shown for different values in the $\zeta_{12D} - \zeta_{22D}$ plane.

which are renormalized in the $\overline{\text{MS}}$ scheme according to

$$\begin{aligned} \delta a_{\chi 1} &= \frac{a_{2D}^2 \zeta_{12D} v^2}{8\pi^2 f_A^2} (3(1 + \zeta_1)\zeta_{12D} + 2\zeta_{22D}) \Delta_{\text{UV}}, \\ \delta a_{\chi 2} &= \frac{3a_{2D}^2 \zeta_{12D}^2 v^2}{8\pi^2 f_A^2} (1 + \zeta_1) \Delta_{\text{UV}}, \\ \delta a_{\chi 3} &= \frac{3a_{2D}^2 \zeta_{12D} v^2}{4\pi^2 f_A^2} [(M_A^2 + M_Z^2)\zeta_{22D} \\ &\quad - 3(M_A^2 + 2M_Z^2)(1 + \zeta_1)\zeta_{12D}] \Delta_{\text{UV}}. \end{aligned} \quad (23)$$

The remaining renormalization of the chiral dimension-2 term follows from Eq. (7)

$$\begin{aligned} \delta \Gamma_2(H(q)H(k_1)H(k_2))|_{\text{div}} \\ = -\frac{9a_{2D}^2 \zeta_{12D}^2}{8\pi^2 f_A^2} \kappa_3 (M_A^2 + m_Z^2) \\ - \frac{a_{2D}^2 \zeta_{12D} M_A^4}{2\pi^2 f_A^2 v} (2(1 + \zeta_1)\zeta_{12D} - \zeta_{22D}). \end{aligned} \quad (24)$$

ATLAS (CMS) have set highly competitive expected 95% confidence level cross section limits of $\sigma/\sigma_{\text{SM}} < 3.9(5.2)$ [28,51] in the $b\bar{b}\tau\tau$ channel [52] alone. Slightly reduced sensitivity [53–55] can be achieved in the $4b$ and $2b2\gamma$ modes [56,57]. ATLAS have combined these channels to obtain a combined exclusion of $3.1\sigma_{\text{SM}}$ [58] with the currently available data and forecast a sensitivity of $\sigma/\sigma_{\text{SM}} \gtrsim 1.1$ at the HL-LHC [59]. We use the two latter result to gain a qualitative sensitivity reach of Higgs pair production in the considered scenario.

In Fig. 4, we show representative invariant Higgs pair mass distributions for 13 TeV LHC collisions, which demonstrates the potential of multi-Higgs final states’ sensitivity to the momentum-enhanced new physics contributions characteristic to the ALP.⁴ The behavior exhibited by the invariant mass distribution is not sensitive to the mass of the ALP as long as the latter is not close to the $\simeq 2M_H$ threshold that determines the $gg \rightarrow HH$ phenomenology. In instances when hefty ALPs propagate freely, their distinctive momentum enhancements will sculpt the Higgs-boson distributions. In parallel, nonlinear effects will be important away from the SM reference point as shown in Fig. 4. This shows that the constraints that can be obtained in the di-Higgs channel are relatively strongly coupled, which is motivation for us to directly include “squared” BSM effects to our analysis in addition to interference effects.

We combine the three representative analyses in a global χ^2 to obtain sensitivity estimates. In the case when the ALP is light, there are significant modifications to Higgs physics, also at large momentum transfers, see also Fig. 4. Of course, these large contributions in particular to the Higgs pair rate are tamed by decreasing signal strengths into SM-like states, which quickly result in tension with experimental observations for larger couplings. As Higgs pair production observations need to rely on relatively clean and high branching ratio final states, the prospects of Higgs pair production (and four top) analyses to provide

⁴We have implemented these changes into an in-house Monte Carlo event generate based on VBFNLO [60,61] employing Feynarts, FormCalc, and LOOPTOOLS [62–65] and PackageX [66] for numerical and analytical cross checks. Throughout this work we chose a renormalization scale of $\mu = 2M_h$.

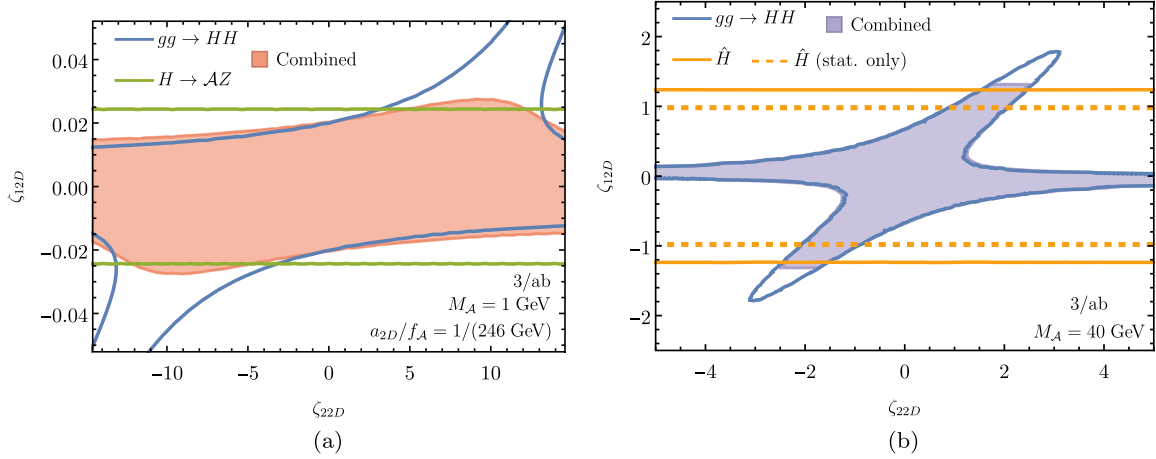


FIG. 5. 95% C.L. regions for the case of a light $M_A = 1$ GeV (left) and heavy $M_A = 40$ GeV (right) ALP.

additional sensitivity is relatively low. This is highlighted already in the combination of the Higgs decay constraints with these processes in Fig. 5(a).

For parameter choices for which the ALP is above the Higgs decay threshold, this picture changes. Multi-Higgs constraints remain relatively insensitive to the ALP mass scale as long as these states are away from the $2M_H$ threshold. The cross section enhancement then translates directly into an enhancement of the observable Higgs boson pair production rate. In turn, constraints on the higher order terms in the ALP flare function become possible. It is important to note that these are independent of couplings (to first order) that shape the ALP decay phenomenology.

As the large enhancements result from the tails of distributions there is a question of validity. Nonetheless the momentum dependence introduced by Eq. (9) leads to partial wave unitarity violation as, e.g., HZ scattering proceeds momentum-enhanced. A numerical investigation shows that for $\mathcal{O}(1)$ couplings in Eq. (8), conserved zeroth partial wave unitarity up to scales ~ 1.5 TeV sets a lower bound of $f_a \gtrsim 300$ GeV for unsuppressed propagation $M_A = 1$ GeV. These constraints are driven by the longitudinal Z polarizations, constraints from transverse modes are comparably weaker. This means that the entire region that is shown in Fig. 4(a) is perturbative at tree-level. In parallel, the HL-LHC is unlikely to probe Higgs pairs beyond invariant masses $M_{HH} > 600$ GeV in the SM (for which the cross section drops to 10% of the inclusive rate). Most sensitivity in HL-LHC searches results from the threshold region. Therefore, the sensitivity expected by the HL extrapolation of [59] will probe Eq. (8) in a perturbatively meaningful regime.

The combined constraints are largely driven by Higgs pair constraints, Fig. 5(a). However, it is worth highlighting that the statistics-only extrapolation does not include changes to the four top search methodology. Improvements of the latter can be expected with

increasing luminosity and the final verdict from four top production might indeed be much more optimistic than our $\sqrt{\text{luminosity}}$ extrapolation might suggest.

V. SUMMARY AND CONCLUSIONS

Searches for new light propagating degrees of freedom such as axionlike particles are cornerstones of the BSM programme in particle physics as explored at, e.g., the Large Hadron Collider. The Higgs boson, since a global picture of its interactions is still incomplete, provides a motivated avenue for the potential discovery of new physics in the near future as the LHC experiments gain increasingly phenomenological sensitivity in rare processes that could be telltale signs of Higgs-related BSM physics.

We take recent experimental developments in multi-Higgs and multitop analyses as motivation to analyse effective Higgs-philic ALP interactions, also beyond leading order. This enables us to tension constraints from different areas of precision Higgs phenomenology, combining Higgs decay modifications with large-momentum transfer processes that are becoming increasingly accessible at the LHC. For light states and sizeable HEFT-like couplings, a large part of the sensitivity is contained in Higgs signal strength measurements (see also [27]), which, however, only provide limited insights into the Higgs-ALP interactions. Higher terms of the Higgs-ALP flare function, still have the phenomenological potential to sizeably modify Higgs pair final states at a level that will be observable at the LHC in the near future. Our findings therefore also highlight further the relevance of multitop and multi-Higgs final state for the quest for new physics.

ACKNOWLEDGMENTS

We thank Dave Sutherland for insightful discussions. C. E. thanks the high-energy physics group (FTAE) at the University of Granada for their hospitality during early

stages of this work. A. is supported by the Leverhulme Trust under grant RPG-2021-031. S. D. B is supported by SRA (Spain) under Grant No. PID2019–106087GB-C21 (10.13039/501100011033), and No. PID2021-128396NB-100/AEI/10.13039/501100011033; by the Junta de Andalucía (Spain) under Grants No. FQM-101, No. A-FQM-467-UGR18, and No. P18-FR-4314 (FEDER); and also with the Newton International Fellowship Alumni follow-on funding 2021/22 under grant

No. AL\221040. C. E. is supported by the STFC under Grant No. ST/T000945/1, the Leverhulme Trust under Grant No. RPG-2021-031, and the Institute for Particle Physics Phenomenology Associateship Scheme. P. S. is supported by the Deutsche Forschungsgemeinschaft under Germany’s Excellence strategy EXC2121 “Quantum Universe”—390833306. This work has been partially funded by the Deutsche Forschungsgemeinschaft (DFG, German Research Foundation)—491245950.

-
- [1] R. D. Peccei and H. R. Quinn, *Phys. Rev. Lett.* **38**, 1440 (1977).
- [2] F. Wilczek, *Phys. Rev. Lett.* **40**, 279 (1978).
- [3] P. W. Graham, I. G. Irastorza, S. K. Lamoreaux, A. Lindner, and K. A. van Bibber, *Annu. Rev. Nucl. Part. Sci.* **65**, 485 (2015).
- [4] I. G. Irastorza and J. Redondo, *Prog. Part. Nucl. Phys.* **102**, 89 (2018).
- [5] J. Jaeckel and M. Spannowsky, *Phys. Lett. B* **753**, 482 (2016).
- [6] F. Esser, M. Madigan, V. Sanz, and M. Ubiali, *J. High Energy Phys.* **09** (2023) 063.
- [7] G. Alonso-Álvarez, J. Jaeckel, and D. D. Lopes, *arXiv:2302.12262*.
- [8] M. Bauer, M. Neubert, S. Renner, M. Schnubel, and A. Thamm, *Phys. Rev. Lett.* **127**, 081803 (2021).
- [9] M. Bauer, M. Neubert, S. Renner, M. Schnubel, and A. Thamm, *J. High Energy Phys.* **09** (2022) 056.
- [10] M. Bauer, M. Neubert, and A. Thamm, *J. High Energy Phys.* **12** (2017) 044.
- [11] A. Biekötter, M. Chala, and M. Spannowsky, *Phys. Lett. B* **834**, 137465 (2022).
- [12] M. Bauer, G. Rostagni, and J. Spinner, *Phys. Rev. D* **107**, 015007 (2023).
- [13] J. Bonilla, I. Brivio, M. B. Gavela, and V. Sanz, *J. High Energy Phys.* **11** (2021) 168.
- [14] G. Buchalla, O. Catà, and C. Krause, *Nucl. Phys.* **B880**, 552 (2014); **B913**, 475(E) (2016).
- [15] G. Buchalla, O. Cata, A. Celis, M. Knecht, and C. Krause, *Nucl. Phys.* **B928**, 93 (2018).
- [16] G. Buchalla, O. Catà, A. Celis, M. Knecht, and C. Krause, *Phys. Rev. D* **104**, 076005 (2021).
- [17] ACME Collaboration, *Nature (London)* **562**, 355 (2018).
- [18] C. Abel, S. Afach, N. J. Ayres, C. A. Baker, G. Ban, G. Bison, K. Bodek, V. Bondar, M. Burghoff, E. Chanel *et al.*, *Phys. Rev. Lett.* **124**, 081803 (2020).
- [19] G. G. Raffelt, *Stars as Laboratories for Fundamental Physics: The Astrophysics of Neutrinos, Axions, and Other Weakly Interacting Particles* (University of Chicago Press, Chicago, 1996), ISBN: 978-0-226-70272-8.
- [20] G. Raffelt and L. Stodolsky, *Phys. Rev. D* **37**, 1237 (1988).
- [21] C. O’Hare, *cajohare/axionlimits: Axionlimits*, <https://cajohare.github.io/AxionLimits/> (2020).
- [22] G. Aad *et al.* (ATLAS Collaboration), *J. High Energy Phys.* **03** (2021) 243; **11** (2021) 50.
- [23] A. M. Sirunyan *et al.* (CMS Collaboration), *Phys. Lett. B* **797**, 134826 (2019).
- [24] D. d’Enterria, in *Workshop on Feebly Interacting Particles* (2021), *arXiv:2102.08971*.
- [25] A. Tumasyan *et al.* (CMS Collaboration), *J. High Energy Phys.* **04** (2022) 087.
- [26] A. M. Sirunyan *et al.* (CMS Collaboration), Technical Report, CERN, Geneva, 2023.
- [27] I. Brivio, M. B. Gavela, L. Merlo, K. Mimasu, J. M. No, R. del Rey, and V. Sanz, *Eur. Phys. J. C* **77**, 572 (2017).
- [28] A. Tumasyan *et al.* (CMS Collaboration), *Phys. Lett. B* **842**, 137531 (2023).
- [29] G. Aad *et al.* (ATLAS Collaboration), *Phys. Rev. D* **108**, 052003 (2023).
- [30] A. Hayrapetyan *et al.* (CMS Collaboration), *arXiv:2305.13439*.
- [31] G. Aad *et al.* (ATLAS Collaboration), *Eur. Phys. J. C* **83**, 496 (2023).
- [32] C. Englert, G. F. Giudice, A. Greljo, and M. McCullough, *J. High Energy Phys.* **09** (2019) 041.
- [33] A. M. Sirunyan *et al.* (CMS Collaboration), *Eur. Phys. J. C* **80**, 75 (2020).
- [34] R. Alonso, M. B. Gavela, L. Merlo, S. Rigolin, and J. Yepes, *Phys. Lett. B* **722**, 330 (2013); **726**, 926(E) (2013).
- [35] I. Brivio, J. Gonzalez-Fraile, M. C. Gonzalez-Garcia, and L. Merlo, *Eur. Phys. J. C* **76**, 416 (2016).
- [36] M. Herrero and R. A. Morales, *Phys. Rev. D* **102**, 075040 (2020).
- [37] M. J. Herrero and R. A. Morales, *Phys. Rev. D* **104**, 075013 (2021).
- [38] Anisha, O. Atkinson, A. Bhardwaj, C. Englert, and P. Stylianou, *J. High Energy Phys.* **10** (2022) 172.
- [39] N. D. Christensen and C. Duhr, *Comput. Phys. Commun.* **180**, 1614 (2009).
- [40] A. Alloul, N. D. Christensen, C. Degrande, C. Duhr, and B. Fuks, *Comput. Phys. Commun.* **185**, 2250 (2014).
- [41] S. Dittmaier *et al.* (LHC Higgs Cross Section Working Group), *Handbook of LHC Higgs Cross Sections: I. Inclusive Observables* (CERN, Geneva, 2011).
- [42] G. Aad *et al.* (ATLAS Collaboration), *J. High Energy Phys.* **07** (2023) 088.

- [43] G. Aad *et al.* (ATLAS Collaboration), Report No. ATL-PHYS-PUB-2018-054, 2018.
- [44] R. Barbieri, A. Pomarol, R. Rattazzi, and A. Strumia, *Nucl. Phys.* **B703**, 127 (2004).
- [45] R. L. Delgado, A. Dobado, and F. J. Llanes-Estrada, *J. High Energy Phys.* **02** (2014) 121.
- [46] I. n. Asiain, D. Espriu, and F. Mescia, *Phys. Rev. D* **105**, 015009 (2022).
- [47] M. J. Herrero and R. A. Morales, *Phys. Rev. D* **106**, 073008 (2022).
- [48] A. Denner, *Fortschr. Phys.* **41**, 307 (1993).
- [49] J. Alwall, R. Frederix, S. Frixione, V. Hirschi, F. Maltoni, O. Mattelaer, H. S. Shao, T. Stelzer, P. Torrielli, and M. Zaro, *J. High Energy Phys.* **07** (2014) 079.
- [50] A. M. Sirunyan *et al.* (CMS Collaboration), Report No. CMS-PAS-FTR-18-031, 2018.
- [51] G. Aad *et al.* (ATLAS Collaboration), *J. High Energy Phys.* **07** (2023) 040.
- [52] M. J. Dolan, C. Englert, and M. Spannowsky, *J. High Energy Phys.* **10** (2012) 112.
- [53] G. Aad *et al.* (ATLAS Collaboration), *Phys. Rev. D* **106**, 052001 (2022).
- [54] A. Tumasyan *et al.* (CMS Collaboration), *Phys. Rev. Lett.* **129**, 081802 (2022).
- [55] A. M. Sirunyan *et al.* (CMS Collaboration), *J. High Energy Phys.* **03** (2021) 257.
- [56] U. Baur, T. Plehn, and D. L. Rainwater, *Phys. Rev. D* **69**, 053004 (2004).
- [57] D. E. Ferreira de Lima, A. Papaefstathiou, and M. Spannowsky, *J. High Energy Phys.* **08** (2014) 030.
- [58] G. Aad *et al.* (ATLAS Collaboration), Report No. ATLAS-CONF-2021-052, 2021.
- [59] G. Aad *et al.* (ATLAS Collaboration), Report No. ATL-PHYS-PUB-2022-053, 2022.
- [60] K. Arnold *et al.*, *Comput. Phys. Commun.* **180**, 1661 (2009).
- [61] J. Baglio *et al.*, [arXiv:1107.4038](https://arxiv.org/abs/1107.4038).
- [62] T. Hahn and M. Perez-Victoria, *Comput. Phys. Commun.* **118**, 153 (1999).
- [63] T. Hahn, *Nucl. Phys. B, Proc. Suppl.* **89**, 231 (2000).
- [64] T. Hahn, *Comput. Phys. Commun.* **140**, 418 (2001).
- [65] T. Hahn and M. Rauch, *Nucl. Phys. B, Proc. Suppl.* **157**, 236 (2006).
- [66] H. H. Patel, *Comput. Phys. Commun.* **218**, 66 (2017).
- [67] D. de Florian *et al.* (LHC Higgs Cross Section Working Group), *Handbook of LHC Higgs Cross Sections: 4. Deciphering the Nature of the Higgs Sector* (CERN, Geneva, 2017), Vol. 2.